# RESOLUTION ENHANCEMENT OF HYPERSPECTRAL IMAGES USING A LEARNING-BASED SUPER-RESOLUTION MAPPING TECHNIQUE

Fereidoun A. Mianji, Member, IEEE, Ye Zhang, Yanfeng Gu

School of Electronics and Information Technique, Harbin Institute of Technology
E-mail: fmianji@ieee.org

*Presenting Author: Yanfeng Gu*

## 1. INTRODUCTION

Many different algorithms for spatial resolution enhancement of hyperspectral (HS) images have been proposed in last decade [1-9]. In a considerable number of proposed methods the spatial information of a high resolution (HR) image is imposed onto the low resolution (LR) HS image [1-4]. Some other approaches are based on spectral mixture analysis (SMA) or subpixel classification [1-7]. Super-resolution mapping (SRM) is a different approach by which the spatial-spectral information of HS images is exploited using an HR image or a model to describe the most likely distribution of the content of mixed pixels [6-10].

The limitations of the mentioned approaches, i.e. high computational cost or the need for supplementary source of information, have been the motivation of the proposed fast and autonomous SRM algorithm for spatial resolution enhancement of HS images.

## 2. LINEAR SPECTRAL UNMIXING

A frequent assumption in HS remote sensing is that spectral signatures result from linear combinations of endmember spectra [11]. These approaches largely ignore the inherent nonlinear characteristics of hyperspectral data [12].

Endmember spectra are endmember components in n-dimensional space. Let $L$ equal the number of endmembers in the spectral library with $l$ ranging from 1 to $L$. Each spectrum in the library consists of $M$ discrete wavelengths ( $\lambda_m$ ) where $m$=1 to $M$. Let $S^l(\lambda_m)$ represent the spectral response of material $l$ at wavelength $\lambda_m$. Each spectrum in the library is described by the following vector:

$$s^l = (S^l(\lambda_1), S^l(\lambda_2), ..., S^l(\lambda_M)) \qquad (1)$$

For an unknown spectra $u = (u_1, u_2, ..., u_M)$ each vector component is composed of a linear combination of $j$ endmembers from $J$. u is related to $J$ by the estimation vector $x = (x_1, x_2, ..., x_L)$ where

$$0 \le x_l \le 1 \quad \text{and} \quad \sum_{l=1}^{L} x_l = 1 \qquad (2)$$

Some algorithms have been developed to handle the linear mixture model (LMM) according both nonnegativity and sum-to-one constraints described by (2). Among them, fully constrained least squares (FCLS) algorithm can efficiently meet both abundance constraints and is optimal in terms of least squares error [13].

## 3. SUPER-RESOLUTION MAPPING (SRM)

The basis for the proposed super-resolution mapping (SRM) technique is spatial correlation of endmembers. It means that any endmember within a pixel tend to be assigned to the subpixels which possess a higher contribution of same endmember in neighboring pixels. The SRM model can be depicted as fig. 1 in which $f_{i,j}^k$ is a pixel of the original LR fractional image and $f(TL)_{i,j}^k$ , $f(TR)_{i,j}^k$ , $f(BL)_{i,j}^k$ , and $f(BR)_{i,j}^k$ are its subpixels.

$$\begin{bmatrix} f_{i-1,j-1}^k & f_{i-1,j}^k & f_{i-1,j+1}^k \\ f_{i,j-1}^k & f_{i,j}^k & f_{i,j+1}^k \\ f_{i+1,j-1}^k & f_{i+1,j}^k & f_{i+1,j+1}^k \end{bmatrix} \xrightarrow{\text{SRM model}} \begin{bmatrix} f_{i,j}^k(TL) & f_{i,j}^k(TR) \\ f_{i,j}^k(BL) & f_{i,j}^k(BR) \end{bmatrix}$$

Fig.1. The SRM model.

## 4. BACKPROPAGATION NEURAL NETWORK (BPNN)

Backpropagation neural network (BPNN) with biases, a sigmoid layer, and a linear output layer are capable of approximating any function with a finite number of discontinuities [14]. Typically, a new input leads to an output similar to the correct output for input vectors used in training that are similar to the new input being presented. This generalization property makes it possible to train a network on a representative set of input/target pairs and get good results without training the network on all possible input/output pairs. Fig. 2 shows a 3 layer BPNN.

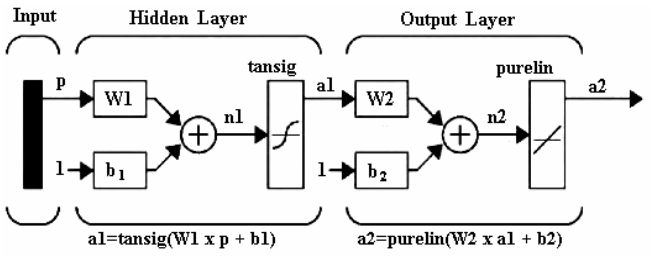


Fig. 2. A three layer BPNN

To improve the performance of the BPNN, a backpropagation learning algorithm with a Fletcher-Reeves version of conjugate gradient is adopted.

## 5. EXPERIMENTAL DESIGN

The test data (Dataset-II) is an AVIRIS-II HS data with 126 available bands in the 0.4–1.8 $\mu$m wavelength range without any available *a priori* knowledge of the landcovers.

The original HS image is used as the high resolution (HR) standard data. First the endmember extraction (using pixel purity index (PPI)) and linear spectral unmixing is applied on the HS image to extract the spatial-spectral information of the landcovers. This is carried out based on the developed LMM and FCLS algorithm. The result of this step is the HR fractional images of the scene. These HR fractional images are the reference images for the algorithm. Then, the original HS image is subsampled by a $2 \times 2$ mean filter in every band. The down-sampled HS image which has the role of LR data in the algorithm, are inputted to the linear spectral unmixing program to result the low resolution (LR) fractional images. Subsampled LR fractional images (by a $2 \times 2$ mean filter) and LR fractional images are used to make the input and target vectors for training of the BPNN, respectively.

## 6. EXPERIMENTS AND RESULTS

The whole algorithm is applied on Dataset-II. After training of the BPNN, LR fractional images are inputted to the SRM algorithm and the spatially enhanced results are compared to the standard images through the RMSE and CC. Fig.3 shows some of the enhanced fractional images and the standard images. Enhancement in the resolution of the images especially on the edges is clear.

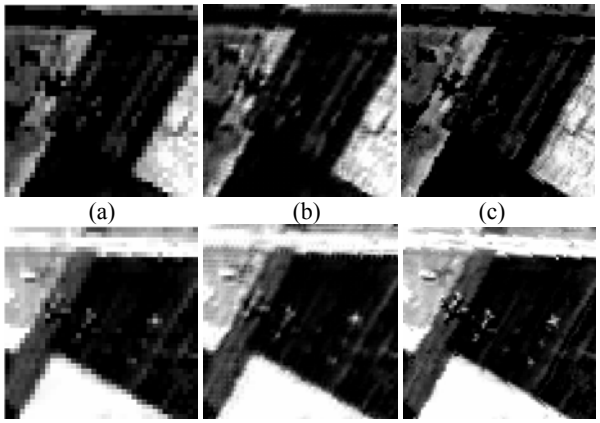

(a) (b) (c)

(d) (e) (f)

Fig. 3. Experimental results on Dataset-II. (a), (b), and (c) the LR, enhanced, and standard images for concrete, respectively. (d), (e), and (f) the LR, enhanced, and standard images for sand, respectively.

Table 1. RMSE and CC values for the enhanced and LR images for some extracted classes of Dataset-II

| | Concrete | Sand |
|---|---|---|
| RMSE of the LR image | 0.0928 | 0.0807 |
| RMSE of the enhanced image | 0.0714 | 0.0641 |
| CC of the LR image | 0.9542 | 0.9816 |
| CC of the enhanced image | 0.9710 | 0.9877 |

RMSE and CC of the LR fractional images in addition to the ones of the enhanced images are depicted in Table 1 to present an evaluation of the method performance.

## 7. CONCLUSION

In this paper a novel resolution enhancement method for HS imagery through SMA and a learning-based SRM technique is proposed. The analysis of the results validates the effectiveness of the method and approves its performance. The technique is fast and independent of the secondary high resolution sources of data. Furthermore, it needs no a priori information about the landcovers of the HS image.

## REFERENCES


[1] G.D. Robinson, H.N. Gross, and J. R. Schott, "Evaluation of two applications of spectral mixing models to image fusion," Remote Sensing of Environment, 71 (3) 272–281, 2000.

[2] M.T. Eismann and R.C. Hardie, "Hyperspectral resolution enhancement using high-resolution multispectral imagery with arbitrary response functions," IEEE Trans. Geosci. Remote. Sens., 43 (3) 455–465, 2005.

[3] H.N. Gross and J.R. Schott, "Application of spectral mixture analysis and image fusion techniques for image sharpening," Remote Sensing of Environment, 63 (2) 85–94, 1998.

[4] M.T. Eismann and R.C. Hardie, "Application of the stochastic mixing model to hyperspectral resolution enhancement," IEEE Trans. Geosci. Remote. Sens., 42 (9) 1924–1933, 2004.

[5] P.M. Atkinson, M.E.J. Cutler, and H. Lewis, "Mapping sub-pixel proportional land cover with AVHRR imagery," Int. J. Remote Sens., 18 (4) 917–935, 1997.

[6] G.M. Foody, "Sharpening fuzzy classification output to refine the representation of sub-pixel land cover distribution," Int. J. Remote Sens., 19 (13) 2593–2599, 1998.

[7] A.J. Tatem, H.G. Lewis, P.M. Atkinson, and M.S. Nixon, "Superresolution target identification from remotely sensed images using a Hopfield neural network," IEEE Trans. Geosci. Remote Sens., 39 (4) 781–796, 2001.

[8] M.Q. Nguyen, P.M. Atkinson, and H.G. Lewis, "Superresolution mapping using a Hopfield neural network with fused images," IEEE Trans. Geosci. Remote Sens., 44 (3) 736–749, 2006.

[9] K.C. Mertens, L.P.C. Verbeke, T. Westra, and R.R. De Wulf, "Subpixel mapping and subpixel sharpening using neural network predicted wavelet coefficients," Remote Sens. Environ., 91 (2) 225–236, 2004.

[10] Y. Gu, Y. Zhang, and J. Zhang, "Integration of spatial-spectral information for resolution enhancement in hyperspectral images," IEEE Trans. Geosci. Remote Sens., 46(5) 1347-1358, 2008.

[11] Penn, B. S., "Using simulated annealing to obtain optimal linear end-member mixtures of hyperspectral data," Computers & Geosciences, vol. 28 pp. 809–817, 2002.

[12] C.M. Bachmann, T.L. Ainsworth, and R.A. Fusina, "Exploiting manifold geometry in hyperspectral imagery," IEEE Trans. Geosci. Remote Sens., 43(3) 441-454, 2005.

[13] D. Heinz and C.I. Chang, "Fully constrained least squares linear spectral mixture analysis method for material quantification in hyperspectral imagery," IEEE Trans. Geosci. Remote Sens., 39(3) 529–545, 2001.

[14] D. E. Rumelhart and J. L. McClelland, Parallel Distributed Processing, Cambridge, MA: MIT Press, Jul. 1987.